Front. Earth Sci. 2024, 18(4): 831–848
https://doi.org/10.1007/s11707-024-1105-2

RESEARCH ARTICLE

Response of forest belt on the south slope of Tianshan Mountains in China to global warming during 1990–2020

Liyuan ZHENG, Yong ZHANG, Chao LU, Wensheng ZHANG, Bo TAN, Lai JIANG, Yanzhen ZHANG, Chengbang AN (✉)

Key Laboratory of Western China's Environmental Systems (Ministry of Education), College of Earth and Environmental Sciences, Lanzhou University, Lanzhou 730000, China

Abstract Mountain vegetation is highly sensitive to changes in climate. Currently, there is no consensus regarding the direction and magnitude of the spatial migration of mountain vegetation in response to climate change. Past studies have reported that climate change promotes upward or downward movement of plant species along an altitude gradient. Based on meteorological data and remote sensing images, this study analyzed the spatial distribution and dynamic trend of mountain altitudinal vegetation belts on the southern slope of the Tianshan Mountains over the past 30 years and discussed the climatic driving factors of these changes. The results showed that the forest belt in this area is unusual because it is embedded in the grassland belt in a patch-like manner and shows discontinuous changes or replacements along the vertical gradient. With the coexistence of warm humidification and warm drying on the southern slope of the Tianshan Mountains, the response of the upper and lower altitudes of the forest belt to climate change was similar, showing a trend of migration to higher-altitude areas. The main climatic factors affecting the migration of the upper and lower altitudes varied spatially. In general, the upper limit of the forest belt had a higher association with precipitation during the vegetative growth season, while the contribution of temperature-related factors to the lower limit of the forest belt was greater.

Keywords Tianshan Mountains, forest belt, spatial migration, altitude limitation, global warming

1 Introduction

Mountain altitudinal vegetation is very sensitive to climate change in the form of global warming (Steinbauer et al., 2018; Hagedorn et al., 2019), as exhibited by the reoccurrence of succession in many areas (Chen et al., 2011; Guo et al., 2018; Elsen et al., 2020; Zu et al., 2021; Rana et al., 2022). The dynamic changes in mountain altitudinal vegetation belts are considered to be the result of climate change (Li et al., 2021; Zhang et al., 2021). In particular, the migration of mountain vegetation to higher altitudes has been studied as a response to global warming (Parmesan and Yohe, 2003; Lenoir et al., 2008; Chen et al., 2011; Hagedorn et al., 2019; Zischg et al., 2021; Zu et al., 2021; Rana et al., 2022), and plant species have been observed migrating to higher altitude in the European Alps (Lamprecht et al., 2018) and the Chimborazo volcano in Ecuador (Morueta-Holme et al., 2015), whereas the migration to lower altitudes can be explained as a response to changes in regional water balance, for example, the altitude of plant species in California decreased significantly (Crimmins et al., 2011). An increase in water resource utilization by vegetation may offset the impact of warming on distribution. However, recent studies have shown that, at different scales, the direction and magnitude of the spatial migration of mountain vegetation in response to climate change is inconclusive. The majority of previous studies have reported that global warming causes plant species to move upward along the altitudinal gradient (Gottfried et al., 2012; Zu et al., 2021), however, studies have also reported the downward movement of plant species along the altitudinal gradient, as observed in the Gongga Mountains of Sichuan where 63.9% of the species moved upward and 22.9% of the species moved downward (Zu et al., 2021).

As unique geographical units, mountain ecosystems exhibit spatial variation in environmental factors owing to changes in altitude, slope, and aspect associated with the

Received March 26, 2023; accepted July 21, 2023

E-mail: cban@lzu.edu.cn

vertical gradient (Zhang et al., 2021). In the context of climate change, mountain vegetation has undergone local extinction and secondary succession, compelling plants to migrate to more suitable habitats (Kelly and Goulden, 2008; Giménez-Benavides et al., 2011) and driving changes in the distribution of vegetation along vertical gradients. In addition, studies have reported that, in different mountain ecosystems, mountain vegetation at different altitude gradients also varies with climate change (Pauli et al., 2012; Zu et al., 2021). Climate change affects the migration of vegetation by altering precipitation and temperature-related climatic factors. For example, the global distribution range of *Aletris spicata* (Thunb.) Franch. was chiefly explained by changes in precipitation, and its altitude range shifted upward by 370 m in the last decades (Zu et al., 2021). Therefore, understanding the spatial and temporal distribution of and dynamic changes in mountain vegetation in different regions and their climatic driving factors is crucial for assessing the impact of climate change on mountain ecosystems.

The Tianshan Mountains, known as the "water tower of Central Asia", provide water sources for major rivers in the arid regions of Central Asia. They are also an important ecological barrier in the arid regions of northwest China (Li et al., 2020) and provide important ecological services for the social and economic development of arid oases (Jiao et al., 2019). Over the past half-century, the temperature increase in the Tianshan Mountains has been higher than the rate of temperature change in the Northern Hemisphere as well as the global increase (Li et al., 2021), and the Tianshan Mountains have shown varying degrees of warming and wetting since the 1980s (Sánchez-González and López-Mata, 2005; Zhang et al., 2022). In addition, as a typical representative of mountain ecosystems in arid regions, not only do these mountains provide a location for human activities but they also perform important carbon sink functions, which are of great importance to the local ecological and economic development, human society, and global carbon cycle (Ni, 2004). However, the response of the Tianshan Mountain ecosystem to global climate change remains unclear. In particular, the response to climate change of vegetation belts at different altitudes on the southern slope of the Tianshan Mountains is still unknown; thus, further research is urgently required. Studies in this field have important scientific implications for environmental protection and monitoring regional and global carbon cycles in the arid region of northwest China. Therefore, this study examined Landsat data from the Google Earth Engine (GEE) cloud platform to analyze altitudinal vegetation belts on the southern slope of the Tianshan Mountains. We aimed to answer the following key questions. 1) What has been the migration trend of the forest belt on the southern slope of the Tianshan Mountains over the past 30 years? 2) How has the forest belt on the southern slope of the Tianshan Mountains responded to climate change?

2 Materials and methods

2.1 Study area

The study area was located in the Tianshan Mountains in Central Asia, near the center of Eurasia (Fig. 1). It spans 1700 km from east to west, with an average elevation of 2300 m. The large mountain system influences the atmospheric circulation in the region, resulting in clear differences in the natural climate between the northern and southern Tianshan Mountains. The southern region has a warm temperate climate, whereas the northern region's climate is temperate. Additionally, this area is affected by westerly winds from the North Atlantic, resulting in a unique humid climate in the Tianshan Mountains, which are also known as the "Central Asian

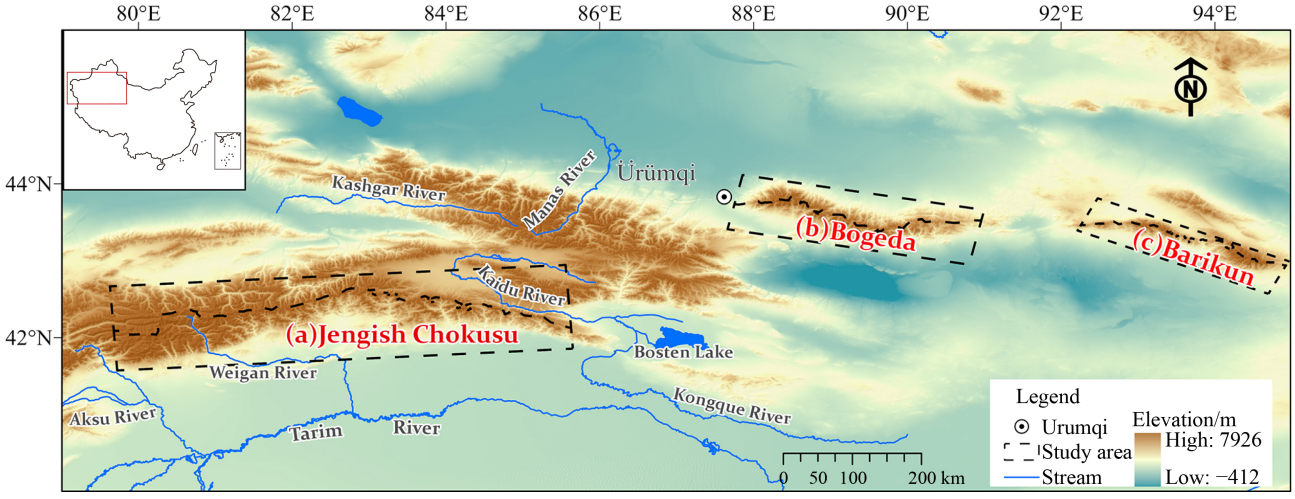

Fig. 1 Location of the study area. (black a, b, and c in the figure represent three study sub-areas).

wet island" (Li et al., 2020; Yue et al., 2020; Zhang et al., 2021). The unique climate of the Tianshan Mountains results in well-developed altitudinal vegetation belts, thereby forming the most representative mountain altitudinal vegetation belt in the temperate arid regions of the world (Zhang et al., 2021). The Tianshan Mountains are composed of a series of east–west parallel mountains and their corresponding basins and valleys. Consideration was given to minimizing the impact of human factors in the selection and division of the study area. Although vegetation change results from the combined effect of climate change and human activities (Ma et al., 2023), global warming is considered the main driver of changes in terrestrial ecosystems (Urban, 2015; Feeley et al., 2020; Trisos et al., 2020; Antão et al., 2022), which determines the survival and distribution of surface vegetation. Therefore, based on the first law of geography that "everything is related to everything else, but near things are more related to each other" (Tobler, 1970), we avoided selecting a study area near the center of human activity in the city. Instead, we focused on three typical mountain ranges (Jengish Chokusu, Bogeda Mountain, and Barikun Mountain, from west to east) on the southern slope of the Tianshan Mountains (Fig. 1) to study the spatial dynamics of altitudinal vegetation belts over the past 30 years. Jengish Chokusu is located near the border between China and Kyrgyzstan, at an elevation of 7443.8 m. It is the highest peak in the Tianshan Mountains and is listed as a national nature reserve. Bogeda Mountain, at an elevation of 5445 m, is one of the most prominent mountains in the western part of the East Tianshan Mountains. Barikun Mountain is one of the most prominent mountains in the eastern section of the East Tianshan Mountains, stretching 160 km, with an average elevation of 3300 m. A large area, including the main peak, was selected for analysis based on the direction of the mountains.

2.2 Data resources

Owing to the rapid development of remote sensing technology and the emergence of the Google Earth Engine (GEE) cloud platform, vegetation cover types can be quickly analyzed with long temporal scales, large spatial scales, and at high spatial resolution (Zurqani et al., 2020). Therefore, from the data provided on the GEE platform, we selected seven-time nodes (1990, 1995, 2000, 2005, 2010, 2015, and 2020) and used the random forest (RF) classification method to divide the vegetation into four types: desert, grassland, forest, and ice–snow. However, five distinct vegetation belts are present in the study region as deserts appear at two altitude ranges simultaneously. According to field investigations, the higher altitude range is considered an alpine desert. Therefore, the spatial distribution of the five altitudinal vegetation belts on the southern slope of the Tianshan Mountains during different periods was obtained.

The remote sensing data used in this study consisted of Landsat Thematic Mapper/Enhanced Thematic Mapper/ Operational Land Imager (TM/ETM/OLI) images from 1990 to 2020 in the Landsat Collection 2 Level-2 data set, which was accessed through GEE. To facilitate the accurate extraction of vegetation belts, the median of the image set was used as a single image with a spatial resolution of 30 m, mainly from the vegetation growth season (June–September), for the specific acquisition time (Fig. 2). The revisit period of Landsat data is 16 days, but it is discontinuous in time due to frequent cloud pollution and other factors. The data loss and stitching completion are shown in Table 1. For the years with missing data or large cloud cover, the image mosaic of adjacent years is used to fill in. The specific method is to first take the research year as the center, and then look for the next year to find whether there is a suitable image. If there is, the image of the year will be used to fill in the holes of the research year. On the contrary, the research year is used as the center to look forward to one year, and finally, a suitable and effective image is obtained.

The China Land Cover Data set (CLCD) contains multi-temporal land use classification data from China, with a spatial resolution of 30 m and a high level of classification accuracy, which can be used as potential training samples (Yang and Huang, 2021). The sample data are mainly based on CLCD, and its spatial distribution is shown in Figs. 3, 4, and 5. Among them, there are 520 samples per period in the Jengish Chokusu,

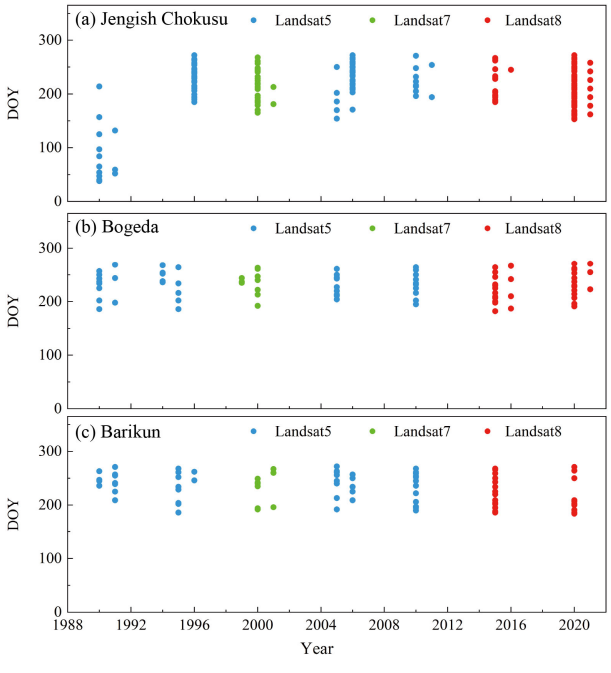

Fig. 2 Landsat image acquisition date. Day of year (DOY), refers to the number of days in a year images were obtained. (a) Jengish Chokusu; (b) Bogeda; (c) Barikun.

Table 1 Data missing and splicing in the study area

Year	Jengish Chokusu	Bogeda	Barikun
1990	The data missing in the lower right corner of the study area is 6422 km^2, accounting for 10.8% of the total area, which is completely filled by the data of the next year.	There are a few holes in the high-altitude area of the study area, which are completely filled by the next year's data.	There are holes in the high-altitude area of the study area and the data in the lower right corner is missing 2888 km^2, accounting for 25.4% of the total area, which is completely filled by the next year.
1995	The data of the study area is completely missing, the next year is completely covered, and the next year's data are used instead.	The missing data in the middle part of the study area is 4542 km^2, accounting for 21.8% of the total area, which is completely filled by the data of the previous year.	The data in the lower right corner of the study area is missing 2514 km^2, accounting for 22.1% of the total area, which is completely filled by the data of the next year.
2000	There are holes in the high-altitude area of the study area, which is completely filled by the data of the next year.	There are holes in the high-altitude area of the study area, which is completely filled by the data of the next year.	There are holes in the high-altitude area of the study area, which is completely filled by the data of the next year.
2005	There is only a small amount of available data in the study area, which is completely filled by the data of the next year.	Completely covered.	The data in the upper left corner of the study area are missing 2613 km^2, accounting for 23.0% of the total area, which is completely filled by the data of the next year.
2010	The data in the upper right corner of the study area is missing 2108 km^2, accounting for 3.5% of the total area, which is completely filled by the data of the next year.	Completely covered.	Completely covered.
2015	The data missing in the lower left corner of the study area is 6457 km^2, accounting for 10.8% of the total area, which is completely filled by the data of the next year.	There is only a small amount of available data in the study area, which is completely filled by the data of the next year.	Completely covered.
2020	There is only a small amount of available data in the study area, which is completely filled by the data of the next year.	There is only a small amount of available data in the study area, which is completely filled by the data of the next year.	Completely covered.

a total of 7 periods; there are 200 samples per period in the Bogeda Mountain, a total of 7 periods; there are 160 samples in each period of Barikun Mountain, a total of 7 periods. In addition, to improve the accuracy of the sample points, Google Earth Pro historical images were used for correction. The selection process of training samples is as follows: First, a certain number of random sample points are generated in the study area, and then the land classification attributes of the sample points are extracted through the CLCD product. Finally, the sample points with errors and fuzzy attributes are eliminated by Google Earth Pro, and the training samples are finally obtained. The historical image tool in Google Earth Pro can view images of different periods, but in fact, Google images are not continuous or homogenous but are mosaicked using multiple images from different periods,

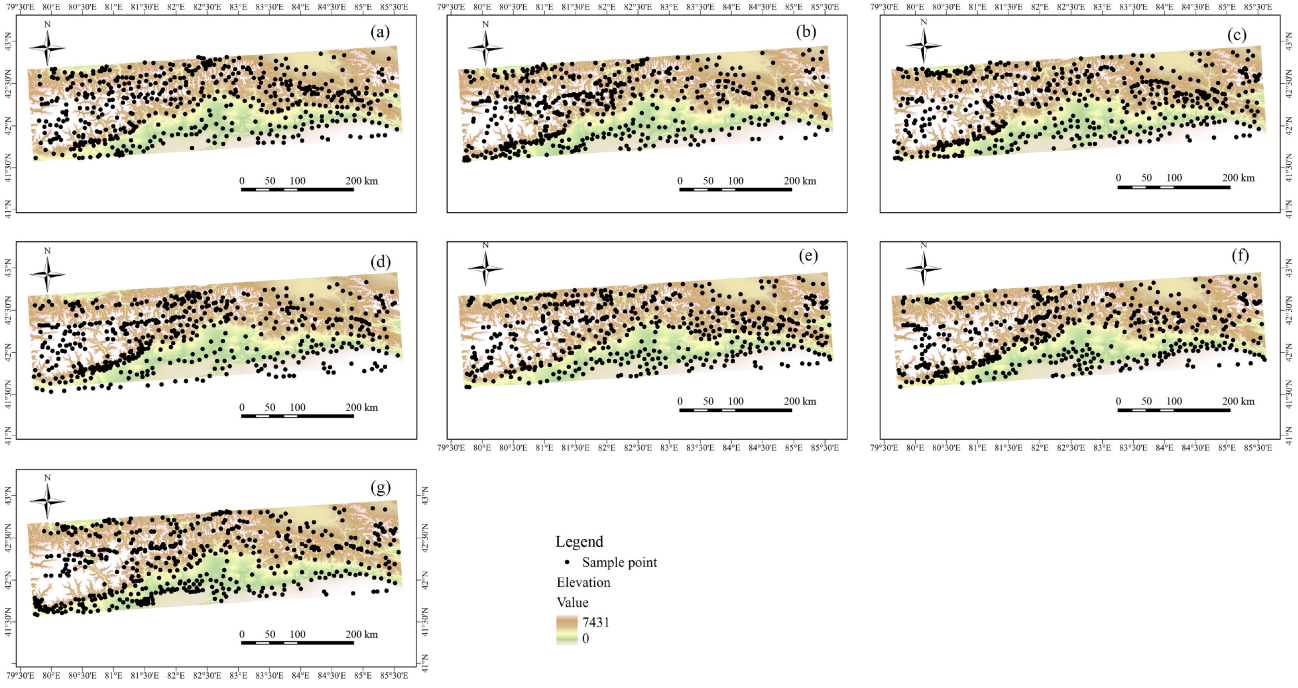

Fig. 3 The spatial distribution of sample data in each period in the Jengish Chokusu region, (a) 1990; (b) 1995; (c) 2000; (d) 2005; (e) 2010; (f) 2015; (g) 2020.

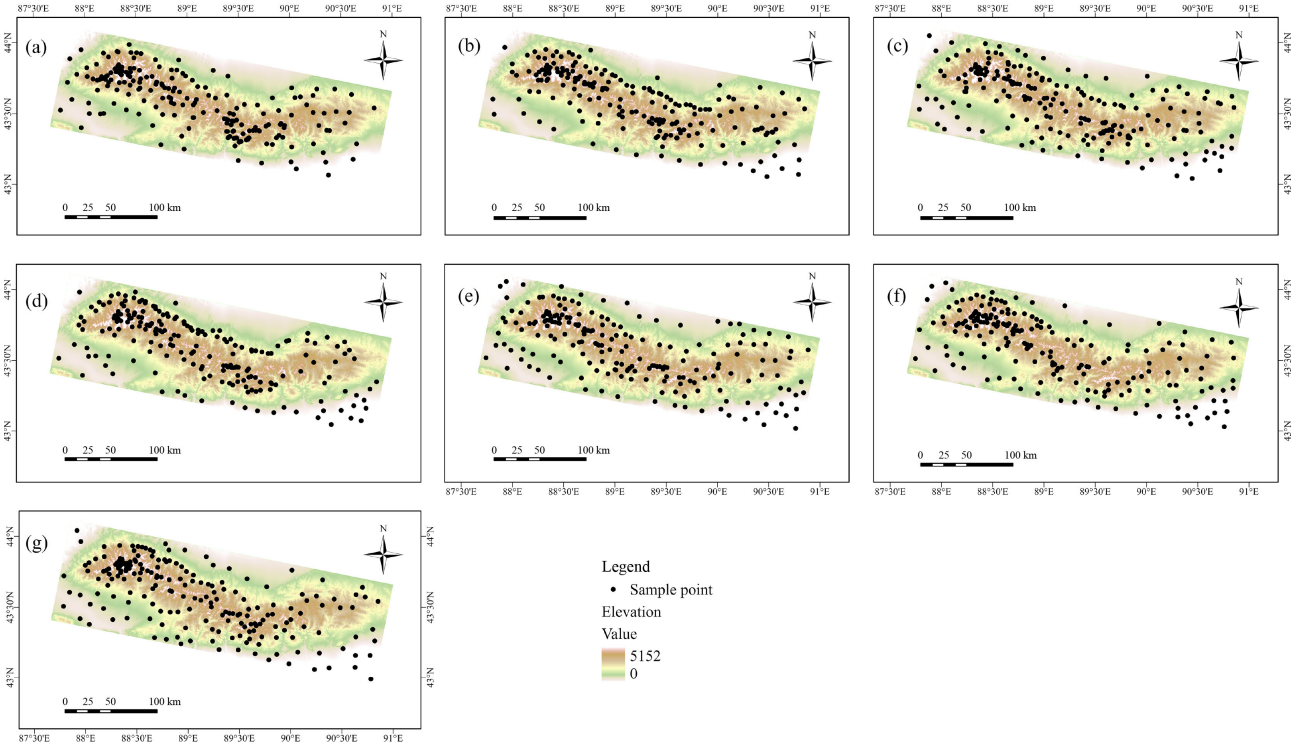

Fig. 4 The spatial distribution of sample data in each period in Bogeda Mountain, (a) 1990 ;(b) 1995; (c) 2000; (d) 2005; (e) 2010; (f) 2015; (g) 2020.

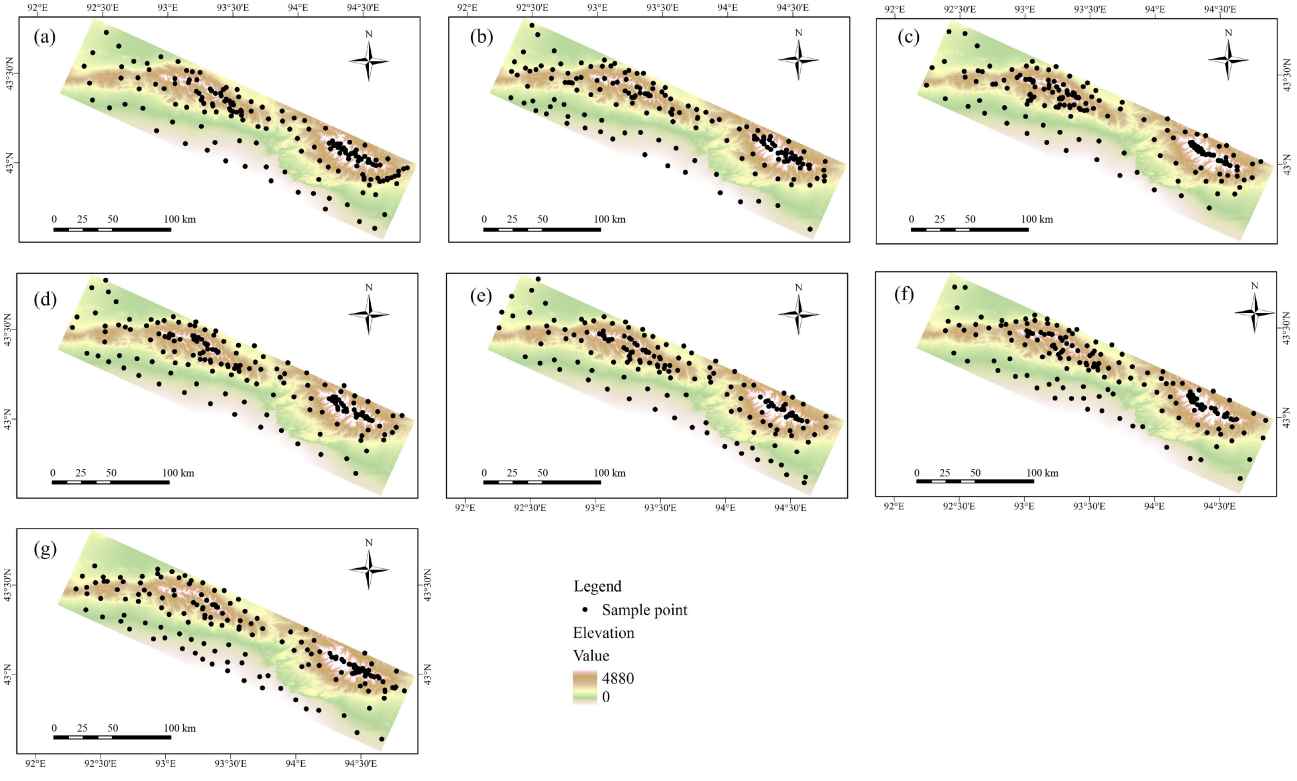

Fig. 5 The spatial distribution of sample data in each period in Barikun Mountain, (a) 1990; (b) 1995; (c) 2000; (d) 2005; (e) 2010; (f) 2015; (g) 2020.

different spatial resolutions, and from different imagery providers (Lesiv et al., 2018; Nwilo et al., 2022). The images are compiled from a wide variety of sources such as SPOT 5, Rapid Eye, Earth Resource Observation Satellites (EROS), Meteosat 2, Geoeye 1, and Digital Globe World View 2 satellite (Buka et al., 2015).

Because Google Earth images come from multiple information sources, they do not have the same spatial resolution (Goudarzi and Landry, 2017). In the correction process, we mainly consider the historical Google Earth images with the highest possible resolution (15 m−10 cm) from 1990 to 2020.

A digital elevation model (DEM) was used to extract the elevation of vegetation, mainly from the Shuttle Radar Topography Mission (SRTM) 30 m spatial resolution DEM data provided in GEE.

Meteorological data included monthly average temperature (Peng, 2019), monthly precipitation (Peng, 2020), and monthly potential evapotranspiration (Peng, 2022). The spatial resolution of the three data is 1 km, and the data format is NetCDF, that is .nc format. These data are mainly used to generate relevant bioclimatic variables. Spatial interpolation data will result in greater uncertainty due to interpolation methods and random errors (Huang et al., 2019). To this end, we use the temperature and precipitation observation data in the Tianshan Mountains to evaluate the accuracy of this interpolated climate data. The interpolation data of temperature and precipitation are significantly correlated with the observation data, indicating that the study of long-term climate trends in the Tianshan Mountains is accurate and effective (Fig. 6). We selected the temperature, precipitation, and potential evapotranspiration data of the National Tibetan Plateau Scientific Data Center from 1990 to 2020.

2.3 Random forest

Random forest (RF) is an ensemble learning method based on a decision tree, which combines several ensemble regression or classification trees (Breiman, 2001a) and uses Bagging or Bootstrap aggregating algorithms to construct numerous different training subsets. Each decision tree provides classification results for samples that are not selected as training samples, and the final class is determined by the highest score (Tian et al., 2016). Owing to the RF method's high prediction accuracy and tolerance to outliers and noise, it is a non-parametric modeling tool with an adaptive function (Breiman, 1996; Yu et al., 2018); thus, it was chosen for this study.

First, an RF algorithm was applied to the classification of remote sensing images in GEE. The characteristic parameters involved in the classification mainly comprised 16 variables. In the classification process, we randomly divide the sample points into a training set of 70% and a validation set of 30%, and then obtain the overall classification accuracy and kappa coefficient to evaluate the classification results. The variables and their importance in the classification process are shown in Tables A1–A3, and the classification accuracy is shown in Tables A4–A6. When using the random forest classification method, we should pay attention to its uncertainty. The uncertainty of the random forest classification method mainly comes from data uncertainty and model uncertainty. The random forest generates multiple training subsets from the original data set through self-sampling, but the data distribution of each subset may be different. This may lead to differences between the trained decision trees, which in turn affects the prediction performance of the random forest. Each decision tree in the random forest is constructed independently, and the features are randomly selected for splitting. The randomness of feature selection can increase the diversity of the model, but it may also lead to

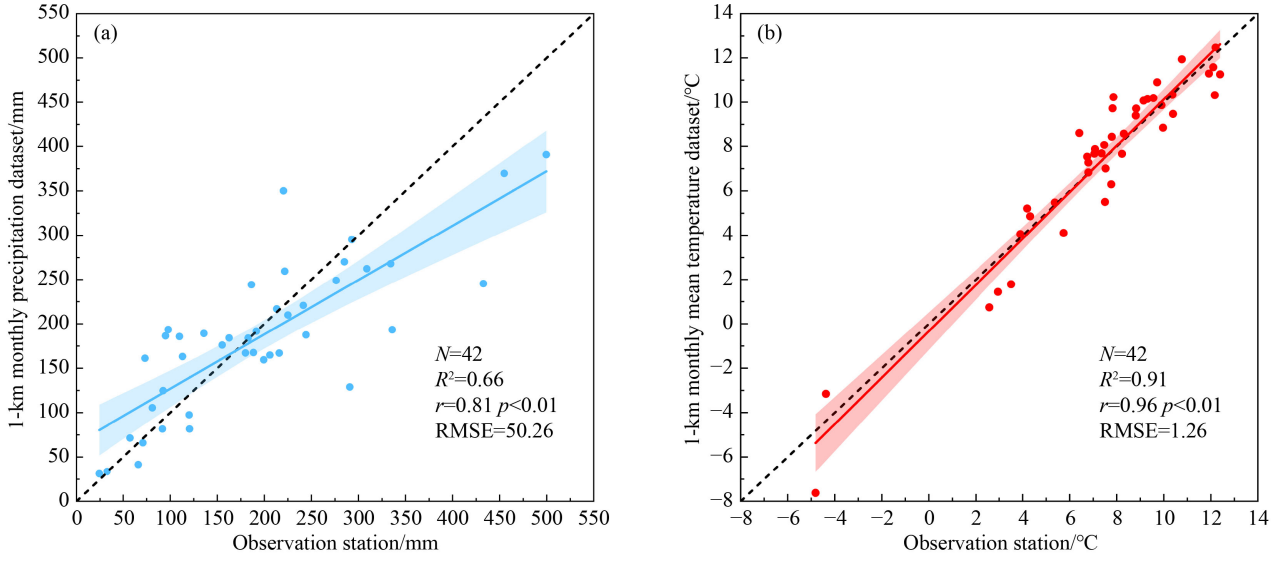

Fig. 6 Comparison of observational climate data and spatial interpolation climate data in Tianshan Mountains. (a) and (b) represent the annual precipitation and annual mean temperature, respectively. The correlation coefficient (r), R^2, P value, and root mean square error (RMSE) were calculated. The dashed line represents the 1:1 reference line, and the solid line represents the regression line. Shadow represents a 95% confidence interval. N represents the number of sites, take 2005 as an example.

the inability of some decision trees to capture key features, making each decision tree capture information slightly different, resulting in model uncertainty. In general, in the process of using random forest classification, multiple tests are required, including the depth of the tree, the selection of classification features, etc., to optimize the performance of the model.

Next, RFs were applied to the regression of vegetation belts in response to climate change and environmental factors. As climate change involves multiple dimensions, the relative importance of different climatic variables differs with vegetation type, space, and time. Asymmetric changes in climatic conditions may lead to complex responses among the species in regional communities (Antão et al., 2022). To evaluate the importance of climate variables, it is important to select biological response variables with known relationships to climate variables (Greenberg et al., 2015), namely bioclimatic variables. Precipitation, temperature, and potential evapotranspiration are known to have a substantial effect on vegetation change (Ma et al., 2023). Based on this understanding, with reference to the WorldClim bioclimatic variables, nine bioclimatic variables were selected for RF regression analysis: annual potential evapotranspiration (APET), annual precipitation (AP), mean annual temperature (MAT), temperature seasonality (TS), precipitation seasonality (PS), precipitation of coldest quarter (PCQ), precipitation of warmest quarter (PWQ), mean temperature of coldest quarter (MTCQ), and mean temperature of warmest quarter (MTWQ). MAT, AP, and APET are very important for forest growth and are widely used in the study of forest growth under the background of climate change (Yu et al., 2014; Zhang et al., 2016; Brandt et al., 2017; Liu et al., 2021). In addition, we used precipitation and temperature in the warmest and coldest seasons (corresponding to growing and non-growing seasons) to characterize the difference between the growing and non-growing seasons. Seasonal temperature and seasonal precipitation are also important factors for the survival and development of organisms (Shrestha et al., 2018; Ge et al., 2019). These bioclimatic variables are calculated based on monthly average temperature (Peng, 2019), monthly precipitation (Peng, 2020), and monthly potential evapotranspiration (Peng, 2022). TS is defined as the amount of temperature variation over a given period based on the ratio of the standard deviation of the monthly mean temperatures to the mean monthly temperature (also known as the coefficient of variation (CV)). PS is a measure of the variation in monthly precipitation totals over the course of the year. This index is the ratio of the standard deviation of the monthly total precipitation to the mean monthly total precipitation (also known as the coefficient of variation). PCQ approximates the total precipitation that prevails during the coldest quarter. PWQ approximates the total precipitation that prevails during the warmest quarter. MTCQ approximates mean temperatures that prevail during the coldest quarter. MTWQ approximates mean temperatures that prevail during the warmest quarter. The response of forest belt with dense vegetation coverage in a typical area of the southern slope of the Tianshan Mountains to climate change was analyzed, and the relative importance of each factor was evaluated using an RF regression model. The important parameters of random forest regression are as follows: the number of trees is 100, the maximum depth of the tree is 10, the maximum depth of the leaves is 50, the minimum number of samples required for the re-division of internal nodes is 2, and the minimum number of samples for leaf nodes is 1. This type of regression analysis has certain limitations in explaining the relationships between variables. Although this model cannot explain whether a causal relationship exists between the variables, it is not hindered by the multicollinearity problem faced by general regression analysis. Furthermore, RF does not require variable selection, which is convenient for calculating the nonlinear effects of variables. Instead, this model reflects the interaction between variables and is suitable for evaluating importance (Breiman, 2001b; Li, 2013; Zhang et al., 2018; Yan et al., 2021). Another factor that we accounted for was the time lag in the response of vegetation dynamics to changes in climate (Zhao et al., 2020). As the spatial migration of mountain vegetation is a long-term process, we averaged the bioclimatic indicators over time to avoid the effect of the response time lag.

2.4 The lower and upper limits of altitudinal vegetation belts

Changes in the spatial distribution of altitudinal vegetation belts are measured by the differences in the lower and upper limits of altitude (Menéndez et al., 2014; Zu et al., 2021). According to our field investigation, altitudes corresponding to 25% and 75% of the maximum number of pixels were set as the lower and upper limits of the vegetation belt, respectively. The upper and lower limits of the forest we extracted refer to the timberline of a closed forest.

3 Results

3.1 Analysis of climate change and spatial distribution of vegetation belts in the study area

Based on meteorological data, we evaluated climate change in three representative mountain regions. The climate records for Jengish Chokusu, Bogeda Mountain, and Barikun Mountain show that over the past 30 years, the three sub-regions experienced discernible climate warming trends (Figs. 7(a)–7(c)), which have passed the

significance test and increasing by (0.031 ± 0.005)°C/yr, (0.021 ± 0.005)°C/yr, and (0.030 ± 0.005)°C/yr, respectively. However, the precipitation fluctuations varied by region (Figs. 7(d)–7(f)). The precipitation in Jengish Chokusu showed an upward trend, increasing by 0.776 ± 0.347 mm/yr. In contrast, the precipitation in Bogeda and Barikun Mountains showed a downward trend, decreasing by 0.842 ± 0.328 mm/yr and 0.932 ± 0.280 mm/yr, respectively, and passed the significance test. Moreover, the seasonal climate records of the three regions show that the study area was warm and humid in summer and cold and dry in winter during the study period (Figs. 7(g)–7(h)). Therefore, the warmest season mentioned in this paper refers to summer, and the coldest season refers to winter.

Based on the random forest classification method, the spatial distribution of vegetation on the southern slope of the Tianshan Mountains was extracted (Figs. 8–10). It was found that the spatial distribution of vegetation in the three study areas is basically the same, and different vegetation belts are radial from the center to the periphery. The ice and snow belt was followed by what we believe to be an alpine desert. This was followed by grassland, forest (which is surrounded by grassland), and lastly desert.The north and south slopes are divided by the ridge line, which is basically symmetric. The forest on the north slope appears in pieces, but the forest on the south slope is more fragmented, also known as spotted. Based

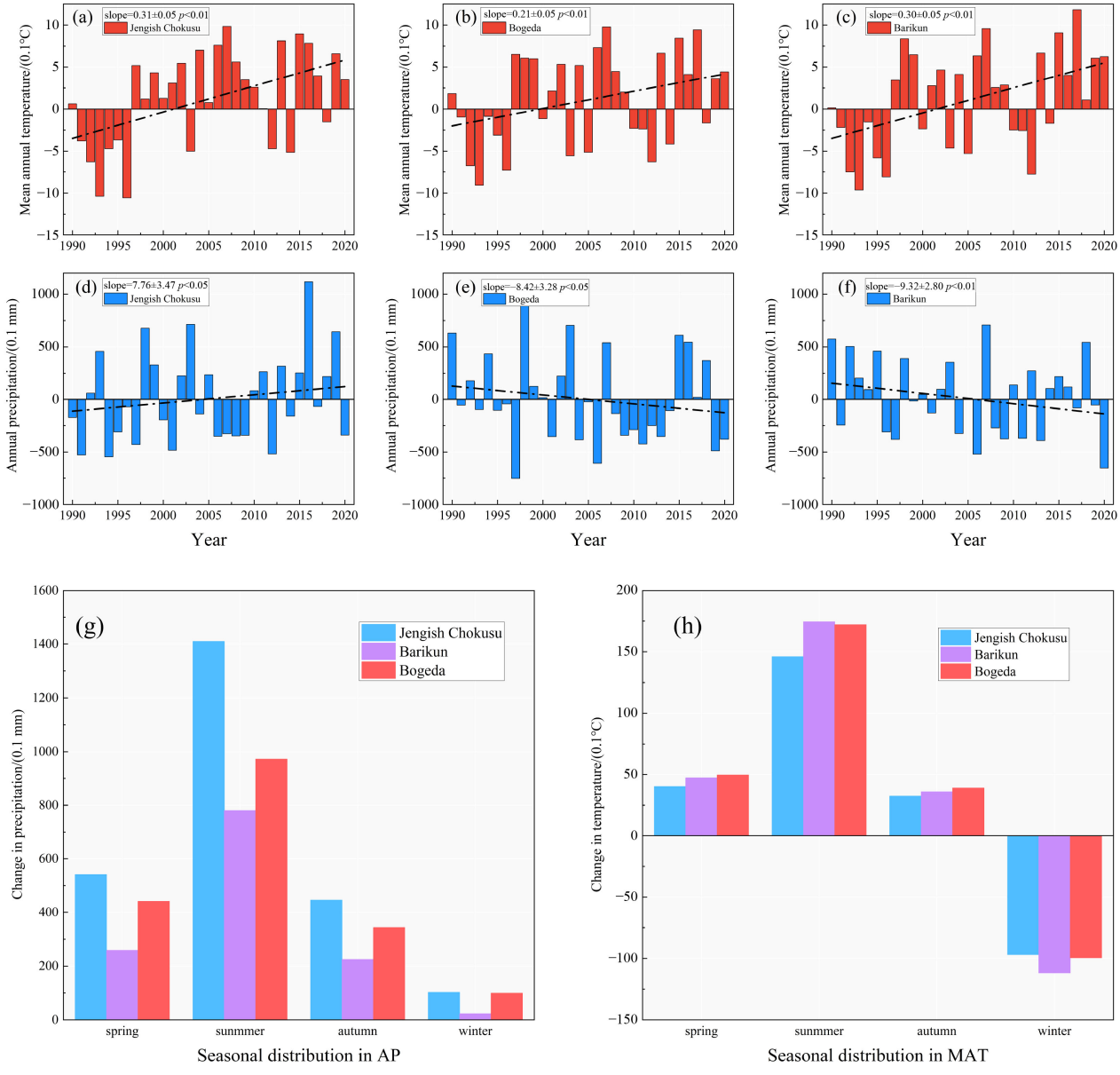

Fig. 7 The changes of mean annual temperature (MAT) in Jengish Chokusu (a), Bogeda Mountain (b), and Barikun Mountain (c) from 1990D to 2020; the change of annual precipitation (AP) in Jengish Chokusu (d), in Bogeda Mountain (e), and in Barikun Mountain (f) from 1990 to 2020; the seasonal distribution of temperature (g) and precipitation (h) in the three regions.

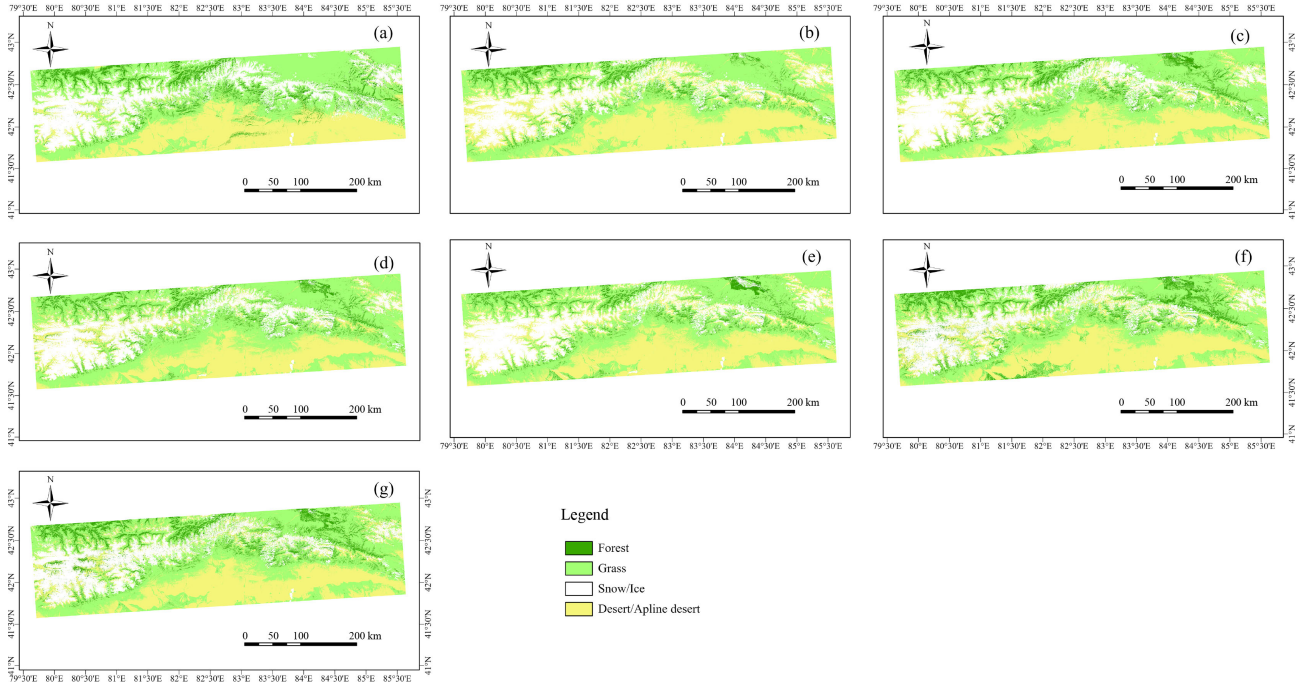

Fig. 8 Spatial results of vegetation classification from 1990 to 2020 in Jengish Chokusu region. (a) 1990; (b) 1995; (c) 2000; (d) 2005; (e) 2010; (f) 2015; (g) 2020.

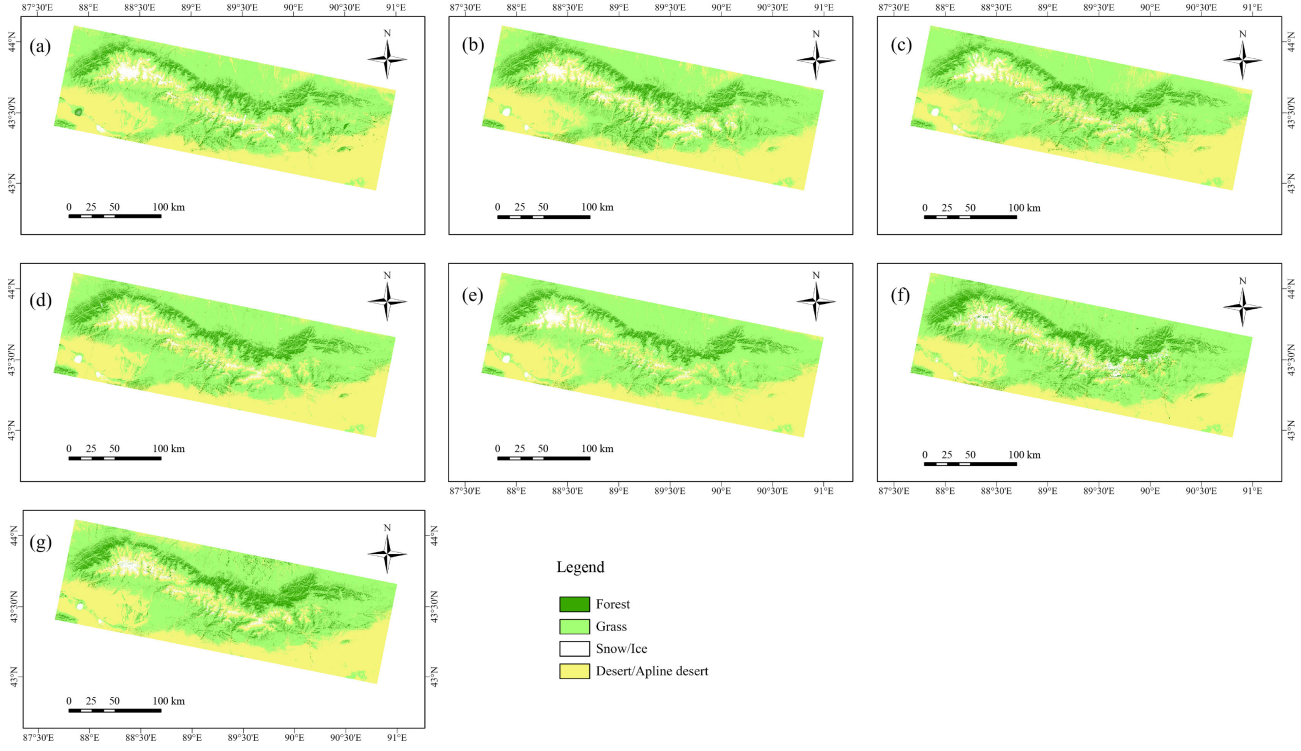

Fig. 9 Spatial results of vegetation classification from 1990 to 2020 in Bogeda Mountain region, (a) 1990; (b) 1995; (c) 2000; (d) 2005; (e) 2010; (f) 2015; (g) 2020.

on the Landsat images, the resolution of these patchy forest areas is at least equal to or greater than 0.009 km^2.

Figure 11 shows that the distribution of altitudinal vegetation belts (represented as pixels on the map) in the three study areas on the southern slope of the Tianshan Mountains was consistent. Moving up the altitude gradient, the land types were: desert, grassland, forest, alpine desert, and ice–snow. A considerable decrease in grassland pixels was observed in areas occupied by forest pixels, indicating that the forest belts were spatially

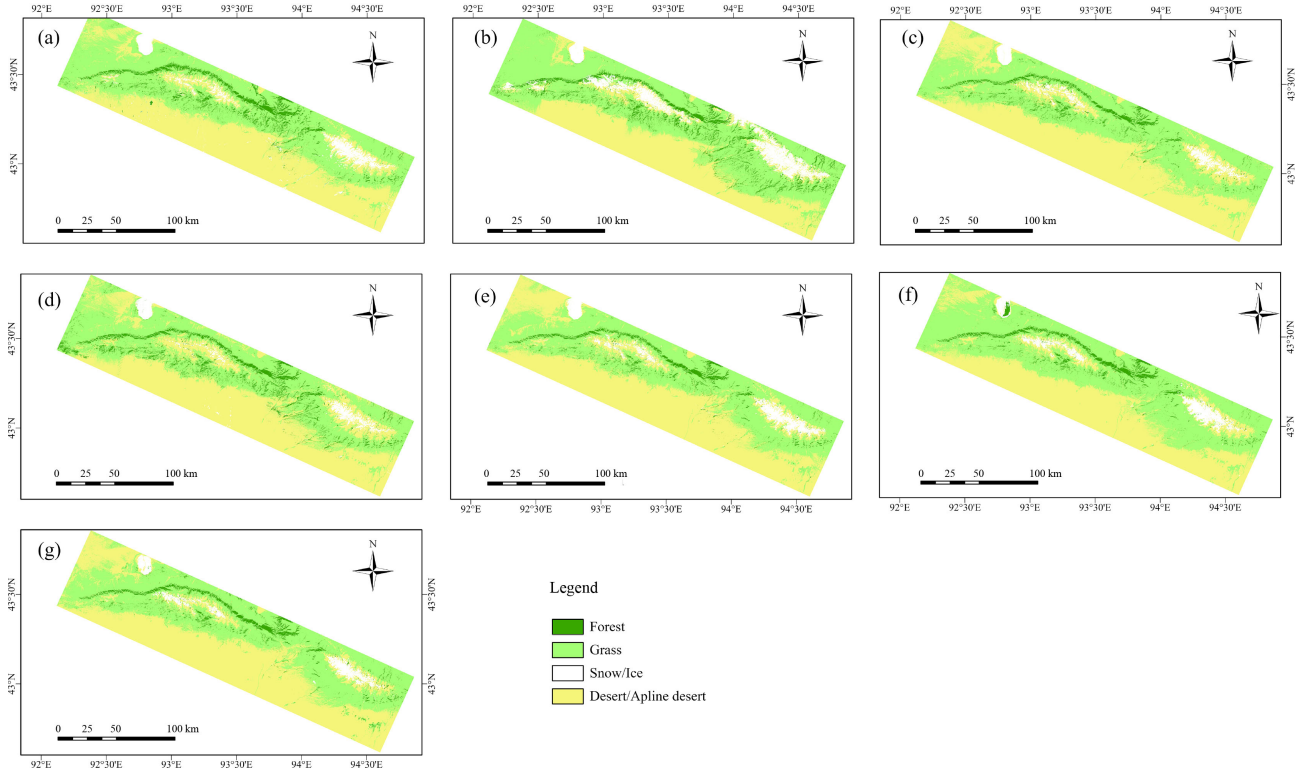

Fig. 10 Spatial results of vegetation classification from 1990 to 2020 in Barikun Mountain region, (a) 1990; (b) 1995; (c) 2000; (d) 2005; (e) 2010; (f) 2015; (g) 2020.

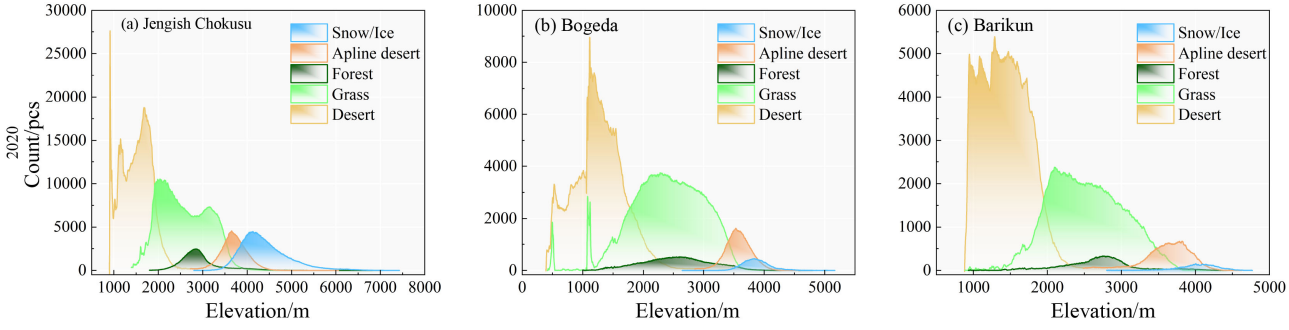

Fig. 11 Changes in the number of pixels with altitude (a–c), (a) Jengish Chokusu; (b) Bogeda Mountains; (c) Barikun Mountain; take 2020 as an example.

distributed within the grassland belt. Forest, alpine desert, and ice–snow belts showed an inverted bell curve similar to the shape of a Gaussian distribution, whereas desert and grassland pixels were more disordered with the altitude distribution curve. In addition, the pixels of each vegetation type clearly coincide with each other, indicating that there was a wide transition area between each vegetation belt. This phenomenon demonstrates the coexistence of different vegetation belts in the same altitude range.

3.2 Variation trend of forest belt in the study area

From the context, it can be seen that the forest belt, as an extremely unique vegetation belt on the southern slope of the Tianshan Mountains, is embedded in the grassland belt in a spot-like manner and shows discontinuous changes or replacements in the vertical gradient, which is different from the previous understanding. From the analysis of the change trend of the upper and lower limits of the typical regional forest belt on the southern slope of the Tianshan Mountains from 1990 to 2020 (Fig. 12), the slope of the trend line of the upper and lower limits of the Jengish Chokusu and the Bogeda Mountain regional forest belt and the lower limit of the Barikun Mountain regional forest belt is greater than 0, and the upper limit of the Barikun Mountain regional forest belt is slightly less than 0, which indicates that the upper and lower limits of the typical regional forest belt on the southern slope of the Tianshan Mountains from 1990 to 2020. The trend of migration in the altitude direction is basically the same. Specifically, the upper limit of the Jengish

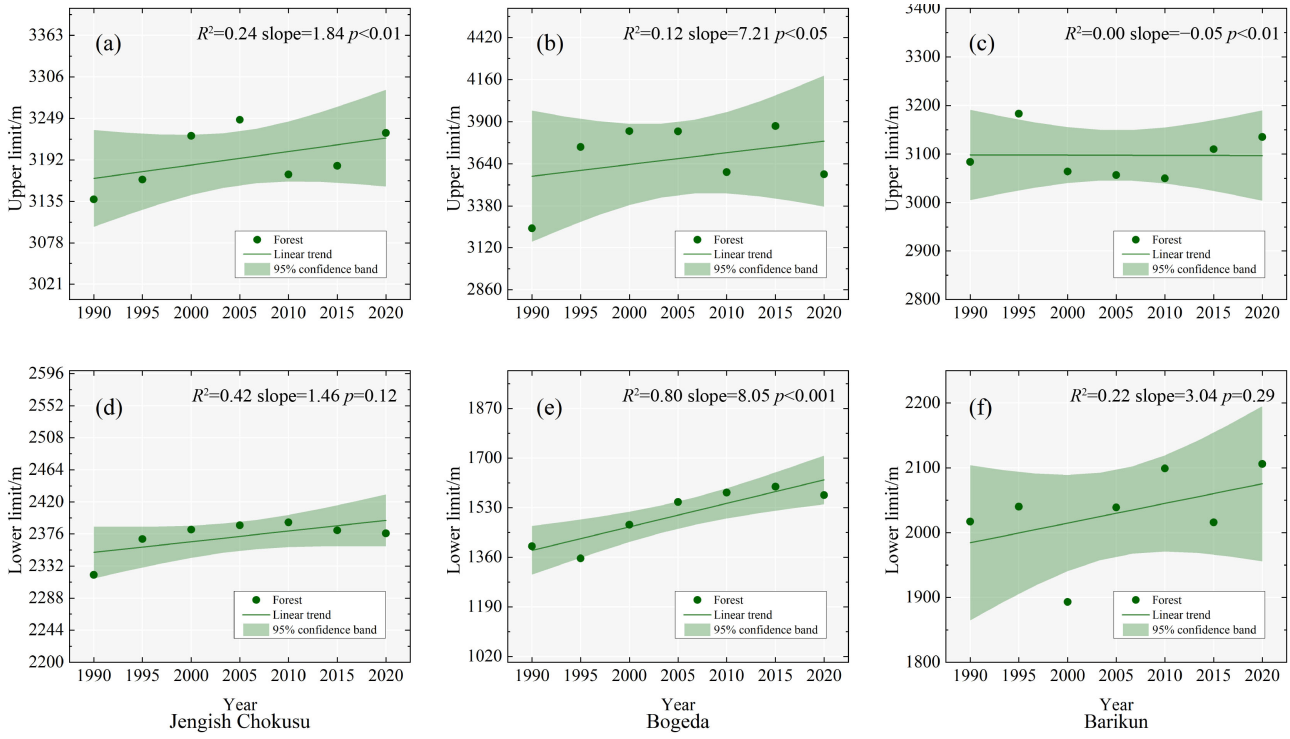

Fig. 12 Changes of the upper and lower limits of the altitude of the forest belt with the year, (a) Jengish Chokusu; (b) Bogeda Mountains; (c) Barikun Mountain.

Chokusu and the Bogeda Mountain regional forest belts on the southern slope of the Tianshan Mountains have migrated to high-altitude areas, while the upper limit of the Barikun Mountain regional forest belt has no obvious trend (a slight downward trend). The changing trend of the lower limit of the forest belt on the southern slope of the Tianshan Mountains was the same, and the three regions showed a trend of migration to high-altitude areas. In addition, for the Jengish Chokusu, the slope of the trend line of the upper and lower limits of the forest belt is greater than 0, and the slope of the trend line of the upper limit is greater than the slope of the lower limit of the forest belt, which indicates that the forest belt is expanding during the overall upward migration of the forest belt in the Jengish Chokusu. For the Bogeda Mountain, the slope of the trend line of the upper and lower limits of the forest belt is greater than 0, and the slope of the trend line of the upper limit is less than the slope of the lower limit of the forest belt, which indicates that the forest belt is shrinking during the overall upward migration of the forest belt in the Bogeda Mountain. For the Barikun Mountain, the slope of the upper limit trend line of the forest belt is close to 0, and the slope of the lower limit trend line is greater than 0, which indicates that the forest belt in the Barikun Mountain is shrinking, and the forest at high altitude is almost unchanged. The main change area is the forest at low altitude. Comparing the three study areas horizontally, it can be found that the slope of the trend line of the Bogeda Mountain is much larger than that of the other two areas, whether it is the upper limit of altitude or the lower limit of altitude, which indicates that the Bogeda Mountain area is the most dramatic area of the Tianshan forest belt. For the upper limit of the forest belt, the Barikun Mountain area is undoubtedly the most stable area; for the lower limit of the forest belt, the slope of the trend line in the T Jengish Chokusu is the smallest, which is the least affected.

3.3 Responses of forest belt to climate change in the study area

As an extremely special forest belt on the southern slope of the Tianshan Mountains, the factors affecting the distribution of the upper and lower limits have spatial differences. From the analysis of the importance of climatic factors affecting the distribution of the upper and lower limits of the forest belt on the southern slope of the Tianshan Mountains (Fig. 13), it can be seen that in the Jengish Chokusu, the most important climatic factor affecting the upper limit of the forest belt is PWQ, followed by AP; the most important climatic factor affecting the lower limit of forest belt is MAT, followed by MTWQ. In the Bogeda Mountains, the most important climate factor affecting the upper limit of the forest belt is MTWQ; the most important climatic factor affecting the lower limit of the forest is AP, followed by MTWQ. In the Barikun Mountains, PWQ is the most important climate factor affecting the upper limit of the forest belt. The most important climatic factor affecting the lower limit of the forest belt is MTCQ. Horizontal comparison,

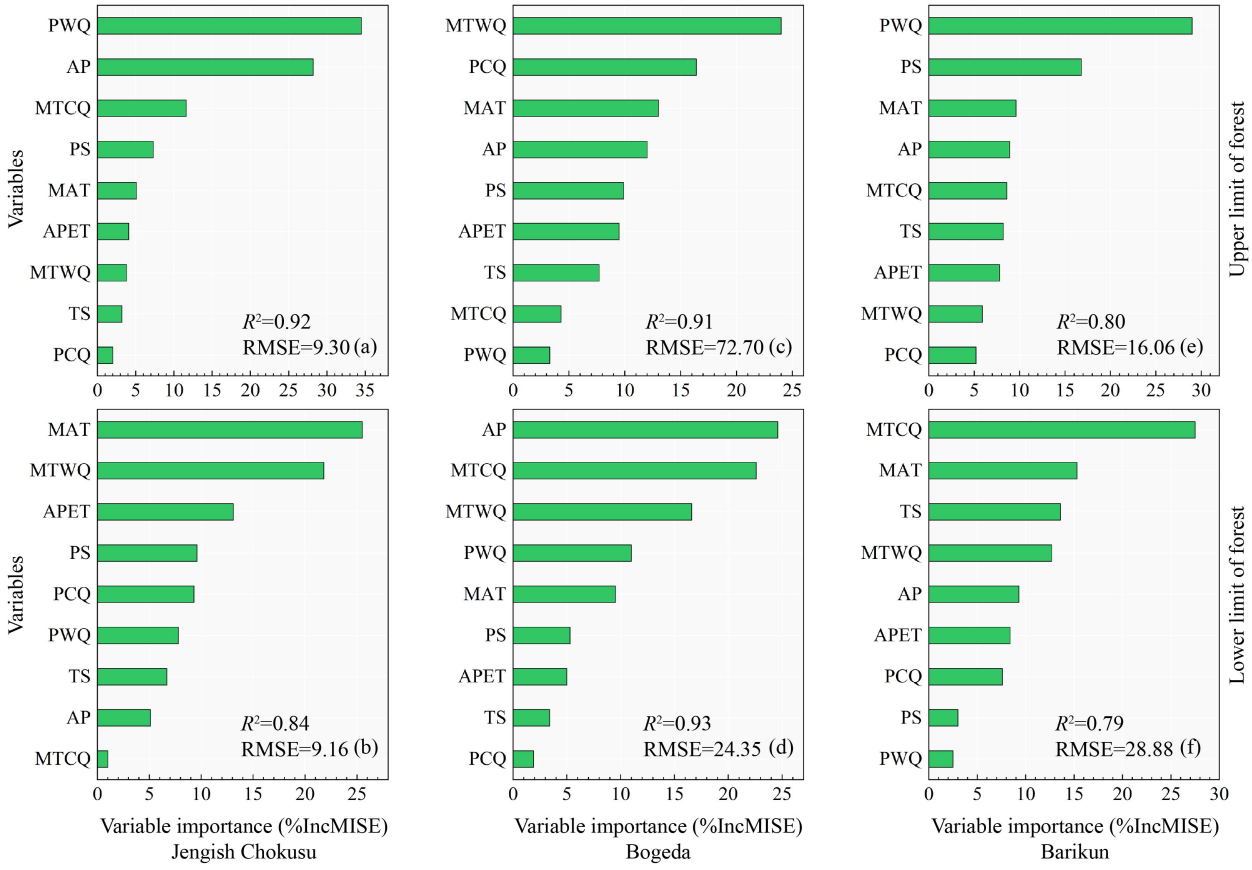

Fig. 13 The upper and lower limits of forest belt altitude are affected by climatic factors. (a) is the upper limit and (b) is the lower limit of the altitude of the forest belt in the Jengish Chokusu; (c) is the upper limit and (d) is the lower limit of the altitude of the forest belt in the Bogeda Mountain; (e) is the upper limit and (f) is the lower limit of the altitude of the forest belt in the Barikun Mountain.

the climatic factors that mainly affect the upper limit of the forest belt in the Jengish Chokusu and the Barikun Mountain are consistent, which is PWQ. The warmest season here corresponds to the growing season, indicating that the precipitation in the growing season is the main factor affecting the upper limit of the forest belt in these two regions. The Bogeda Mountain is different from the previous two regions. The climate factor that mainly affects the upper limit of the forest belt is MTWQ. Similarly, the warmest season here corresponds to the growing season, but the main factor is the MAT, and PWQ is no longer important. The climatic factors affecting the lower limit of the forest belt in Jengish Chokusu, Bogeda Mountain, and Barikun Mountain are very obvious, followed by MAT, AP, and MTCQ.

4 Discussion

4.1 Comparison of responses in forest belt to climate change

Mountain vegetation is extremely sensitive to climate change and mainly relies on the succession of vegetation types to adapt. Mountains have a characteristic vegetation distribution that transitions from deserts, forests, and grasslands to permanently covered snow belts (Hagedorn et al., 2019). The response patterns of the upper and lower altitudes of vegetation belts with different vegetation cover to climate change vary, which leads to the complexity of spatial vegetation migration (Grytnes et al., 2014; Dolezal et al., 2016). Climatic factors drive vegetation changes, especially in the arid regions of north-west China, where ecosystems are fragile and sensitive to climate change. The forest belt on the southern slope of the Tianshan Mountains displays an unusual distribution pattern. Our investigation revealed that the forest is embedded in the grassland belt in the form of patches, showing discontinuous changes or replacements on the vertical gradient. As a plant community, forests should have suitable climatic conditions. Changes in cold, warm, dry, and wet climates directly or indirectly affect the geographical distribution of forests.

The examination of meteorological data showed that the climate in the Jengish Chokusu area had a warming and wetting trend, whereas the climate in the two sub-areas of Bogeda Mountain and Barikun Mountain showed a warming and drying trend. Climate warming is common

in these three regions, yet they differ in moisture level between dry and wet climates. The trend of warming-wetting and warming-drying is significant. Although they have different climatic backgrounds, the response trends of the upper and lower limits of the forest belts in these areas to climate change were similar. The upper and lower limits of the altitude of the Jengish Chokusu and Bogeda Mountain forest belts, and the lower limit of the altitude of the Barikun Mountain forest belt tended to migrate to higher-altitude areas. Notably, the upper limit of altitude in the Barikun Mountain forest belt did not show a distinct trend. We concluded that the migration of the forest belt to the higher-altitude area on the southern slope of the Tianshan Mountains was similar to the current species migration.

4.2 Primary factors affecting changes in forest belts

The migration of vegetation to higher-altitude areas is an adaptation to climate warming (Parmesan and Yohe, 2003; Lenoir et al., 2008; Chen et al., 2011; Morueta-Holme et al., 2015; Hagedorn et al., 2019; Zischg et al., 2021; Zu et al., 2021; Rana et al., 2022), but this phenomenon does not imply that temperature is the primary factor leading to the migration of forest belts to higher altitudes. The limiting effects of other variables, such as water availability, are also very important (Greenberg et al., 2015; Villén-Peréz et al., 2020), and they may contribute more than temperature in some cases. An increase in water use efficiency may offset the effects of warming. The dry and wet climate in this region does not directly represent the actual use of water resources in the ecosystem. For example, on the southern slope of the Tianshan Mountains, numerous glaciers in the high-altitude ecosystem are present, and climate warming will lead to an increase in glacial-melt water in the region. However, another consideration is the highly abundant precipitation levels typically found at higher altitudes. Therefore, the main factors affecting the migration of the upper and lower limits of altitude in the three typical forest belts in this region should be investigated further. In addition, vegetation type, which is mainly related to the biological characteristics of the dominant vegetation, is also one of the factors affecting the migration of the vegetation belt in response to climate change.

From the random forest regression model, it can be found that the relative importance of the PWQ in the Jengish Chokusu and Barikun Mountains is the highest, while the relative importance of the MTWQ in the Bogeda Mountains is the highest. However, if taken together, the PWQ contributes the most, and the warmest season corresponds to the growing season. Therefore, the upper limit of the forest belt on the southern slope of the Tianshan Mountains is more correlated with the precipitation in the vegetation growing season. At the lower limit of the forest belt, the relative importance of the MAT in the Jengish Chokusu is the highest, and the relative importance of the MTCQ in the Barikun Mountain is the highest, all of which are the largest contribution of temperature-related factors, while the relative importance of the AP in the Bogeda Mountain is the highest, followed by the MTCQ. Similarly, on the whole, the largest contribution is the MTCQ and the MTWQ. Therefore, the lower limit of the forest belt on the southern slope of the Tianshan Mountains is more affected by temperature-related factors. The response of the forest belt to climate varies at different altitudes. In low-altitude areas, temperature-related factors contribute the most, while in high-altitude areas, precipitation in the warmest season contributes more. Attention should be paid to the prerequisites. The warmest season already represents temperature-related factors. The migration of vegetation belts is the result of many factors, not the result of a single condition. By comparing the upper and lower limits of the forest belt, it can be found that the temperature-related factor is the primary condition for the migration of the forest belt. With the increase in altitude, the effect of precipitation gradually becomes prominent, and sufficient precipitation in the growing season is conducive to the growth of trees. In general, the higher the altitude, the lower the temperature. Under the background of climate warming, the migration of forest belts to high altitudes is to resist the impact of climate warming. High-altitude areas are more sensitive to climate change (Li et al., 2019; Zheng et al., 2021; Mohd et al., 2022) before trees begin to grow, they also need to reach a certain accumulated temperature (Wang et al., 2013). When the temperature conditions are met, the precipitation factor is highlighted. On the contrary, the sensitivity of low-altitude areas to climate change is reduced, so it may cover up the role of some factors.

5 Conclusions

The response of mountain altitudinal vegetation belts to climate change is mainly reflected by the succession of the dominant vegetation. The forest belt is an extremely unique vegetation belt on the southern slope of the Tianshan Mountains owing to the fact that it is embedded in the grassland belt in the form of patches. Under different climatic backgrounds in different regions on the southern slope of the Tianshan Mountains, the response of the upper and lower limits of the forest belt to climate change is almost the same, showing migration to high-altitude areas, but the main climatic factors affecting the migration of the upper and lower limits are different and have spatial differences. The upper limit of the forest belt is more affected by the precipitation-related factors in the warmest season (corresponding to the growing season). With lower limits of the forest belt, the contribution of temperature-related factors is greater.

As an important ecological barrier and development support in the arid region of northwest China, especially in the southern slope of the Tianshan Mountains, the forest belt migrating to high altitude is expected to break the original carbon balance, and climate change brings multiple uncertainties to it. Under the background of 'double carbon', this will be one of the main research directions in the future.

Acknowledgments This study was supported by grants from the National Natural Science Foundation of China (Grant Nos. 42071102 and 42220104001). The Landsat satellite image used in the study can be obtained from the Google Earth Engine. The meteorological data we use can be obtained from the China Qinghai-Tibet Plateau Scientific Data Center.

Competing interests The authors declare that they have no competing interests.

References

Antão L H, Weigel B, Strona G, Hällfors M, Kaarlejärvi E, Dallas T, Opedal Ø H, Heliölä J, Henttonen H, Huitu O, Korpimäki E, Kuussaari M, Lehikoinen A, Leinonen R, Lindén A, Merilä P, Pietiäinen H, Pöyry J, Salemaa M, Tonteri T, Vuorio K, Ovaskainen O, Saastamoinen M, Vanhatalo J, Roslin T, Laine A L (2022). Climate change reshuffles northern species within their niches. Nat Clim Chang, 12(6): 587–592

Breiman L (1996). Bagging predictors. Mach Learn, 24(2): 123–140

Breiman L (2001a). Random forests. Mach Learn, 45(1): 5–32

Breiman L (2001b). Statistical modeling: the two cultures. Qual Eng, 48: 81–82

Buka L, Maruziva R, Nenhowe P (2015). A comparison of Google Earth extracted points with GPS surveyed points. Ethiop J Environ Stud Manag, 8(5): 484–493

Chen I C, Hill J K, Ohlemüller R, Roy D B, Thomas C D (2011). Rapid range shifts of species associated with high levels of climate warming. Science, 333(6045): 1024–1026

Crimmins S M, Dobrowski S Z, Greenberg J A, Abatzoglou J T, Mynsberge A R (2011). Changes in climatic water balance drive downhill shifts in plant species' optimum elevations. Science, 331(6015): 324–327

Dolezal J, Dvorsky M, Kopecky M, Liancourt P, Hiiesalu I, Macek M, Altman J, Chlumska Z, Rehakova K, Capkova K, Borovec J, Mudrak O, Wild J, Schweingruber F (2016). Vegetation dynamics at the upper elevational limit of vascular plants in Himalaya. Sci Rep, 6(1): 24881

Elsen P R, Monahan W B, Merenlender A M (2020). Topography and human pressure in mountain ranges alter expected species responses to climate change. Nat Commun, 11(1): 1974

Feeley K J, Bravo-Avila C, Fadrique B, Perez T M, Zuleta D (2020). Climate-driven changes in the composition of New World plant communities. Nat Clim Chang, 10(10): 965–970

Ge J, Berg B, Xie Z (2019). Climatic seasonality is linked to the occurrence of the mixed evergreen and deciduous broad-leaved forests in China. Ecosphere, 10(9): e02862

Giménez-Benavides L, Albert M J, Iriondo J M, Escudero A (2011). Demographic processes of upward range contraction in a long-lived Mediterranean high mountain plant. Ecography, 34(1): 85–93

Gottfried M, Pauli H, Futschik A, Akhalkatsi M, Barančok P, Benito Alonso J L, Coldea G, Dick J, Erschbamer B, Fernández Calzado M´ R, Kazakis G, Krajči J, Larsson P, Mallaun M, Michelsen O, Moiseev D, Moiseev P, Molau U, Merzouki A, Nagy L, Nakhutsrishvili G, Pedersen B, Pelino G, Puscas M, Rossi G, Stanisci A, Theurillat J P, Tomaselli M, Villar L, Vittoz P, Vogiatzakis I, Grabherr G (2012). Continent-wide response of mountain vegetation to climate change. Nat Clim Chang, 2(2): 111–115

Goudarzi M A, Landry R Jr. (2017). Assessing horizontal positional accuracy of Google Earth imagery in the city of Montreal, Canada. Geodesy Cartogr, 43(2): 56–65

Greenberg J A, Santos M J, Dobrowski S Z, Vanderbilt V C, Ustin S L (2015). Quantifying environmental limiting factors on tree cover using geospatial data. PLoS One, 10(2): e0114648

Grytnes J-A, Kapfer J, Jurasinski G, Birks H H, Henriksen H, Klanderud K, Odland A, Ohlson M, Wipf S, Birks H J B (2014). Identifying the driving factors behind observed elevational range shifts on European mountains. Global Eco Biogeograph, 23: 876–884

Guo F, Lenoir J, Bonebrake T C (2018). Land-use change interacts with climate to determine elevational species redistribution. Nat Commun, 9(1): 1315

Hagedorn F, Gavazov K, Alexander J M (2019). Above- and belowground linkages shape responses of mountain vegetation to climate change. Science, 365(6458): 1119–1123

Huang J, Jing C, Fu J, Huang Z (2019). Uncertainty analysis of rainfall spatial interpolation in urban small area. In: Gao H, Yin Y, Yang X, Miao H, eds. Testbeds and Research Infrastructures for the Development of Networks and Communities. Cham: Springer International Publishing, 79–95

Jiao L, Jiang Y, Zhang W, Wang M, Wang S, Liu X (2019). Assessing the stability of radial growth responses to climate change by two dominant conifer trees species in the Tianshan Mountains, northwest China. For Ecol Manage, 433: 667–677

Kelly A E, Goulden M L (2008). Rapid shifts in plant distribution with recent climate change. Proc Natl Acad Sci, 105: 11823–11826

Lamprecht A, Semenchuk P R, Steinbauer K, Winkler M, Pauli H (2018). Climate change leads to accelerated transformation of high-elevation vegetation in the central Alps. New Phytol, 220(2): 447–459

Brandt L A, Benscoter A M, Harvey R, Speroterra C, Bucklin D, Romañach S S, Watling J I, Mazzotti F J (2017). Comparison of climate envelope models developed using expert-selected variables versus statistical selection. Ecol Modell, 345: 10–20

Lenoir J, Gégout J C, Marquet P A, de Ruffray P, Brisse H (2008). A significant upward shift in plant species optimum elevation during the 20th century. Science, 320(5884): 1768–1771

Lesiv M, See L, Laso Bayas J C, Sturn T, Schepaschenko D, Karner M, Moorthy I, McCallum I, Fritz S (2018). Characterizing the spatial and temporal availability of very high resolution satellite imagery in Google Earth and Microsoft Bing Maps as a source of

reference data. Land (Basel), 7(4): 118

Li L, Zhang Y, Wu J, Li S, Zhang B, Zu J, Zhang H, Ding M, Paudel B (2019). Increasing sensitivity of alpine grasslands to climate variability along an elevational gradient on the Qinghai-Tibet Plateau. Sci Total Environ, 678: 21–29

Li X (2013). Using random forest for classification and regression. Chinese J App Entomo, 50(4): 1190–1197

Li Y, Chen Y, Li Z (2020). Climate and topographic controls on snow phenology dynamics in the Tienshan Mountains, Central Asia. Atmos Res, 236: 104813

Li Y, Chen Y, Sun F, Li Z (2021). Recent vegetation browning and its drivers on Tianshan Mountain, Central Asia. Ecol Indic, 129: 107912

Liu V, Wang Y, Wang Y, Guo J, Yu P, Wang L, Yu S, Liu F (2021). Separating meteorological condition and soil moisture controls on the variation in stand evapotranspiration of a larch plantation during three hydrological years. Glob Ecol Conserv, 27: e01548

Ma M, Wang Q, Liu R, Zhao Y, Zhang D (2023). Effects of climate change and human activities on vegetation coverage change in northern China considering extreme climate and time-lag and accumulation effects. Sci Total Environ, 860: 160527

Menéndez R, González-Megías A, Jay-Robert P, Marquéz-Ferrando R (2014). Climate change and elevational range shifts: evidence from dung beetles in two European mountain ranges. Glob Ecol Biogeogr, 23(6): 646–657

Morueta-Holme N, Engemann K, Sandoval-Acuña P, Jonas J D, Segnitz R M, Svenning J C (2015). Strong upslope shifts in Chimborazo's vegetation over two centuries since Humboldt. Proc Natl Acad Sci USA, 112(41): 12741–12745

Mohd Z, Zhou W, Wu C, Lin Y, Azeez P A, Song Q, Liu Y, Zhang Y, Lu Z, Sha L (2022). Soil heterotrophic respiration in response to rising temperature and moisture along an altitudinal gradient in a subtropical forest ecosystem, southwest China. Sci Total Environ, 816: 151643

Ni J (2004). Forest productivity of the Altay and Tianshan Mountains in the dryland, northwestern China. For Ecol Manage, 202(1–3): 13–22

Nwilo P C, Okolie C J, Onyegbula J C, Arungwa I D, Ayoade O Q, Daramola O E, Orji M J, Maduako I D, Uyo I I (2022). Positional accuracy assessment of historical Google Earth imagery in Lagos State, Nigeria. Applied Geomatics, 14(3): 545–568

Parmesan C, Yohe G (2003). A globally coherent fingerprint of climate change impacts across natural systems. Nature, 421(6918): 37–42

Pauli H, Gottfried M, Dullinger S, Abdaladze O, Akhalkatsi M, Alonso J L B, Coldea G, Dick J, Erschbamer B, Calzado R F, Ghosn D, Holten J I, Kanka R, Kazakis G, Kollár J, Larsson P, Moiseev P, Moiseev D, Molau U, Mesa J M, Nagy L, Pelino G, Puşcaş M, Rossi G, Stanisci A, Syverhuset A O, Theurillat J P, Tomaselli M, Unterluggauer P, Villar L, Vittoz P, Grabherr G (2012). Recent plant diversity changes on Europe's mountain summits. Science, 336(6079): 353–355

Peng S (2019) 1-km monthly mean temperature dataset for china (1901–2021). In: National Tibetan Plateau Data C, ed. National Tibetan Plateau Data Center

Peng S (2020) 1-km monthly precipitation dataset for China (1901–2021). In: National Tibetan Plateau Data C, ed. National Tibetan Plateau Data Center

Peng S (2022) 1 km monthly potential evapotranspiration dataset in China (1990–2021). In: National Tibetan Plateau Data C, ed. National Tibetan Plateau Data Center

Rana S K, Rana H K, Stöcklin J, Ranjitkar S, Sun H, Song B (2022). Global warming pushes the distribution range of the two alpine 'glasshouse' Rheum species north- and upwards in the Eastern Himalayas and the Hengduan Mountains. Front Plant Sci, 13: 925296

Sánchez-González A, López-Mata L (2005). Plant species richness and diversity along an altitudinal gradient in the Sierra Nevada, Mexico. Divers Distrib, 11(6): 567–575

Shrestha N, Su X, Xu X, Wang Z (2018). The drivers of high Rhododendron diversity in south-west China: Does seasonality matter. J Biogeogr, 45(2): 438–447

Steinbauer M J, Grytnes J A, Jurasinski G, Kulonen A, Lenoir J, Pauli H, Rixen C, Winkler M, Bardy-Durchhalter M, Barni E, Bjorkman A D, Breiner F T, Burg S, Czortek P, Dawes M A, Delimat A, Dullinger S, Erschbamer B, Felde V A, Fernández-Arberas O, Fossheim K F, Gómez-García D, Georges D, Grindrud E T, Haider S, Haugum S V, Henriksen H, Herreros M J, Jaroszewicz B, Jaroszynska F, Kanka R, Kapfer J, Klanderud K, Kühn I, Lamprecht A, Matteodo M, di Cella U M, Normand S, Odland A, Olsen S L, Palacio S, Petey M, Piscová V, Sedlakova B, Steinbauer K, Stöckli V, Svenning J C, Teppa G, Theurillat J P, Vittoz P, Woodin S J, Zimmermann N E, Wipf S (2018). Accelerated increase in plant species richness on mountain summits is linked to warming. Nature, 556(7700): 231–234

Tian S, Zhang X, Tian J, Sun Q (2016). Random forest classification of wetland landcovers from multi-sensor data in the arid region of Xinjiang, China. Remote Sens (Basel), 8(11): 954

Tobler W R (1970). A computer movie simulating urban growth in the detroit region. Econ Geogr, 46: 234–240

Trisos C H, Merow C, Pigot A L (2020). The projected timing of abrupt ecological disruption from climate change. Nature, 580(7804): 496–501

Urban M C (2015). Accelerating extinction risk from climate change. Science, 348(6234): 571–573

Villén-Peréz S, Heikkinen J, Salemaa M, Mäkipää R (2020). Global warming will affect the maximum potential abundance of boreal plant species. Ecography, 43(6): 801–811

Wang Y, Gao L, Zhao X (2013). Tree-ring width chronology of *Populus tremula* and its relationship with the weather in Changbai Mountain of northeastern China. J Northeast Fores U, 41(1): 10–13

Yang J, Huang X (2021). The 30 m annual land cover dataset and its dynamics in China from 1990 to 2019. Earth Syst Sci Data, 13(8): 3907–3925

Yan X J, Chen X H, Ma C C, Cai Y, Cui Z, Chen X, Wu L, Zhang F (2021). What are the key factors affecting maize yield response to and agronomic efficiency of phosphorus fertilizer in China. Field Crops Res, 270: 108221

Yu J, Wang C, Wan J, Han S, Wang Q, Nie S (2014). A model-based method to evaluate the ability of nature reserves to protect

endangered tree species in the context of climate change. For Ecol Manage, 327: 48–54

Yu Y, Li M, Fu Y (2018). Forest type identification by random forest classification combined with SPOT and multitemporal SAR data. J For Res, 29(5): 1407–1414

Yue X, Liu G, Chen J, Zhou C (2020). Synergistic regulation of the interdecadal variability in summer precipitation over the Tianshan mountains by sea surface temperature anomalies in the high-latitude Northwest Atlantic Ocean and the Mediterranean Sea. Atmos Res, 233: 104717

Zhang Y, Liu L y, Liu Y, Zhang M, An C (2021). Response of altitudinal vegetation belts of the Tianshan Mountains in northwestern China to climate change during 1989–2015. Sci Rep, 11(1): 4870

Zhang Y, An C B, Liu L Y, Zhang Y Z, Lu C, Zhang W S (2022). High-elevation landforms are experiencing more remarkable wetting trends in arid Central Asia. Adv Clim Chang Res, 13(4): 489–495

Zhang M G, Slik J, Ma K P (2016). Using species distribution modeling to delineate the botanical richness patterns and phytogeographical regions of China. Sci Rep, 6(1): 22400

Zhang J, Zhang N, Liu Y X, Zhang X, Hu B, Qin Y, Xu H, Wang H, Guo X, Qian J, Wang W, Zhang P, Jin T, Chu C, Bai Y (2018). Root microbiota shift in rice correlates with resident time in the field and developmental stage. Sci Chn Life Sci, 61(6): 613–621

Zhao J, Huang S, Huang Q, Wang H, Leng G, Fang W (2020). Time-lagged response of vegetation dynamics to climatic and teleconnection factors. Catena, 189: 104474

Zheng L, Gaire N P, Shi P (2021). High-altitude tree growth responses to climate change across the Hindu Kush Himalaya. J Plant Ecol, 14(5): 829–842

Zischg A P, Frehner M, Gubelmann P, Augustin S, Brang P, Huber B (2021). Participatory modelling of upward shifts of altitudinal vegetation belts for assessing site type transformation in Swiss forests due to climate change. Appl Veg Sci, 24(4): e12621

Zu K, Wang Z, Zhu X, Lenoir J, Shrestha N, Lyu T, Luo A, Li Y, Ji C, Peng S, Meng J, Zhou J (2021). Upward shift and elevational range contractions of subtropical mountain plants in response to climate change. Sci Total Environ, 783: 146896

Zurqani H A, Post C J, Mikhailova E A, Cope M P, Allen J S, Lytle B A (2020). Evaluating the integrity of forested riparian buffers over a large area using LiDAR data and Google Earth Engine. Sci Rep, 10(1): 14096

AUTHOR BIOGRAPHIES

Liyuan ZHENG received her B.Sc. degree in geographic information science in 2021 from Lanzhou University and is currently conducting M.S. related research at Lanzhou University, China. His major field of study is climate change and environmental remote sensing in arid regions.

His email address is zhengly21@lzu.edu.cn.

Yong ZHANG received his M.S. degree from Gansu Agricultural University, China, in 2018, and is currently conducting Ph.D. related research at Lanzhou University, China. His research interests are climate change and environmental remote sensing in arid regions.

His email address is zhangyong19@lzu.edu.cn.

Chao LU received his B.Sc. degree in cultural relics and museum science from Lanzhou University in 2017, and a M.S. degree in archeology in 2020. Currently, he is a doctoral candidate in the School of Resources and Environment of Lanzhou University. His research interests include archeology and environmental archeology.

His email address is luch20@lzu.edu.cn.

Wensheng ZHANG is a Ph.D. student in palynology and Quaternary environmental change at Lanzhou University in China. He is passionate about the evolution and change of the Earth's environment, especially the climate change and human activities of the past few thousand years. He is currently using palynology techniques to study the environmental evolution process of the arid regions in central Asia, and exploring the response mechanisms of the ecosystem over the past few thousand years.

His email address is zhangwsh20@lzu.edu.cn.

Bo TAN is a Ph.D. student at Lanzhou University in China. His research direction is environmental evolution, and he is mainly engaged in research on the relationship between environmental change and human activities.

His email address is tanging0815@163.com.

Lai JIANG is currently conducting M.S. related research at Lanzhou University, China.

His email address is 220220949361@lzu.edu.cn.

Yan-zhen ZHANG received her B.Sc. degree in geography in 2020 from Lanzhou University. Her major field of study is climate change.

Her email address is zhangyzh2020@lzu.edu.cn.

Chengbang AN is a professor of Lanzhou University and is a doctoral supervisor. The main research direction is environmental change and environmental archeology. He is currently the Deputy Director of the Environmental Change and Environmental Archaeology Committee of the Chinese Geographical Society, and the Deputy Director of the Interglacial Climate and Environment Committee of the Chinese Quaternary Scientific Research Society.

His email address is cban@lzu.edu.cn.

Appendices

Table A1 Importance of characteristic variables of Jengish Chokusu

Characteristic variable	1990	1995	2000	2005	2010	2015	2020
ASPECT [a)]	4.7%	2.9%	2.1%	1.6%	2.4%	1.2%	1.4%
EVI [b)]	7.7%	5.1%	10.2%	7.9%	7.5%	7.5%	5.2%
NDMI [c)]	4.6%	9.1%	6.1%	12.7%	6.2%	6.2%	7.4%
NDSI [d)]	7.0%	7.0%	6.1%	6.0%	4.1%	6.8%	7.8%
NDVI [e)]	6.0%	9.0%	8.6%	9.5%	9.7%	11.1%	8.6%
NDWI [f)]	3.8%	6.4%	6.5%	7.7%	7.9%	6.8%	3.7%
SI-T [g)]	5.1%	7.7%	8.5%	10.7%	10.4%	7.2%	7.9%
SLOPE [h)]	5.7%	3.8%	2.3%	2.8%	3.1%	0.4%	1.7%
SR_B1 [i)]	4.7%	4.7%	4.8%	4.3%	4.0%	6.1%	4.2%
SR_B2 [j)]	5.6%	4.7%	7.2%	3.8%	6.0%	5.9%	10.7%
SR_B3 [k)]	6.5%	5.5%	7.1%	5.2%	6.4%	2.7%	8.8%
SR_B4 [l)]	5.5%	4.9%	3.2%	1.8%	3.6%	6.8%	7.6%
SR_B5 [m)]	5.2%	5.8%	4.9%	7.3%	8.8%	1.0%	3.4%
SR_B7 [n)]	6.1%	9.1%	8.4%	9.9%	8.9%	10.4%	3.4%
ST_B6 [o)]	5.6%	8.8%	7.7%	6.4%	4.6%	7.8%	5.6%
Elevation [p)]	16.3%	5.6%	6.4%	2.6%	6.6%	12.2%	12.6%

Notes: a) ASPECT: Terrain aspect; b) EVI: Enhanced vegetation index; c) NDMI: Normalized difference moisture index; d) NDSI: Normalized difference snow index; e) NDVI: Normalized difference vegetation index; f) NDWI: Normalized Difference Water Index; g) SI-T: Integrated salinity index; h) SLOPE: Terrain aspect; i) SR_B1: Band 1 surface reflectance; j) SR_B2: Band 2 surface reflectance; k) SR_B3: Band 3 surface reflectance; l) SR_B4: Band 4 surface reflectance; m) SR_B5: Band 5 surface reflectance; n) SR_B7: Band 7 surface reflectance; o) ST_B6: Band 6 surface temperature (The Landsat 8 is the 10th band); p) Elevation: Sea-level elevation.

Table A2 Importance of characteristic variables of Bogeda

Characteristic variable	1990	1995	2000	2005	2010	2015	2020
ASPECT [a)]	2.90%	2.30%	0.80%	1.40%	0.50%	0.90%	2.00%
EVI [b)]	7.00%	5.20%	7.00%	6.30%	6.70%	9.90%	9.50%
NDMI [c)]	9.20%	7.60%	11.30%	5.80%	5.10%	8.10%	7.40%
NDSI [d)]	6.20%	4.60%	5.70%	8.10%	5.30%	6.30%	6.20%
NDVI [e)]	6.60%	11.90%	11.70%	12.10%	15.20%	11.70%	8.70%
NDWI [f)]	5.30%	6.80%	6.60%	9.50%	5.70%	5.70%	10.10%
SI-T [g)]	9.40%	12.40%	9.90%	7.40%	13.70%	8.50%	12.00%
SLOPE [h)]	2.80%	3.50%	1.50%	2.90%	0.20%	2.90%	1.00%
SR_B1 [i)]	6.50%	7.30%	4.20%	8.10%	10.00%	6.10%	7.20%
SR_B2 [j)]	4.30%	8.20%	6.70%	5.00%	7.40%	5.90%	7.20%
SR_B3 [k)]	5.60%	6.20%	7.30%	6.80%	8.00%	4.70%	2.90%
SR_B4 [l)]	2.80%	3.30%	1.80%	3.30%	1.50%	6.90%	5.60%
SR_B5 [m)]	6.10%	5.10%	6.40%	4.60%	6.50%	1.10%	1.90%
SR_B7 [n)]	10.90%	5.30%	6.40%	7.40%	7.20%	10.60%	7.00%
ST_B6 [o)]	6.20%	6.00%	8.30%	8.20%	5.50%	5.90%	8.20%
Elevation [p)]	8.20%	4.30%	4.30%	3.20%	1.50%	4.80%	3.10%

Notes: a) ASPECT: Terrain aspect; b) EVI: Enhanced vegetation index; c) NDMI: Normalized difference moisture index; d) NDSI: Normalized difference snow index; e) NDVI: Normalized difference vegetation index; f) NDWI: Normalized Difference Water Index; g) SI-T: Integrated salinity index; h) SLOPE: Terrain aspect; i) SR_B1: Band 1 surface reflectance; j) SR_B2: Band 2 surface reflectance; k) SR_B3: Band 3 surface reflectance; l) SR_B4: Band 4 surface reflectance; m) SR_B5: Band 5 surface reflectance; n) SR_B7: Band 7 surface reflectance; o) ST_B6: Band 6 surface temperature (The Landsat 8 is the 10th band); p) Elevation: Sea-level elevation.

Table A3 Importance of characteristic variables of Barikun

Characteristic variable	1990	1995	2000	2005	2010	2015	2020
ASPECT [a)]	2.6%	2.8%	0.0%	2.5%	1.8%	0.2%	1.2%
EVI [b)]	6.0%	5.7%	7.7%	7.3%	7.0%	13.2%	7.9%
NDMI [c)]	8.1%	9.8%	6.4%	11.2%	8.2%	5.8%	6.8%
NDSI [d)]	8.3%	6.4%	9.3%	6.4%	8.9%	5.9%	6.5%
NDVI [e)]	10.4%	8.1%	11.3%	11.9%	11.8%	12.8%	14.3%
NDWI [f)]	8.3%	6.5%	1.9%	7.0%	6.8%	10.0%	9.2%
SI-T [g)]	12.1%	12.9%	16.8%	8.8%	15.9%	14.3%	11.1%
SLOPE [h)]	2.4%	3.0%	0.8%	3.7%	1.6%	0.9%	1.4%
SR_B1 [i)]	7.5%	5.4%	6.8%	4.5%	5.7%	6.1%	6.2%
SR_B2 [j)]	5.1%	4.1%	7.0%	5.0%	3.9%	7.4%	6.3%
SR_B3 [k)]	6.4%	6.2%	8.1%	5.1%	7.7%	6.9%	6.4%
SR_B4 [l)]	1.7%	2.4%	1.9%	2.7%	2.8%	5.9%	6.4%
SR_B5 [m)]	3.8%	7.4%	8.1%	5.5%	4.2%	4.4%	2.8%
SR_B7 [n)]	9.2%	9.5%	4.5%	6.8%	6.0%	1.4%	4.6%
ST_B6 [o)]	5.1%	5.2%	5.3%	6.0%	4.2%	2.8%	5.0%
Elevation [p)]	3.1%	4.9%	4.1%	5.4%	3.4%	2.2%	3.9%

Notes: a) ASPECT: Terrain aspect; b) EVI: Enhanced vegetation index; c) NDMI: Normalized difference moisture index; d) NDSI: Normalized difference snow index; e) NDVI: Normalized difference vegetation index; f) NDWI: Normalized Difference Water Index; g) SI-T: Integrated salinity index; h) SLOPE: Terrain aspect; i) SR_B1: Band 1 surface reflectance; j) SR_B2: Band 2 surface reflectance; k) SR_B3: Band 3 surface reflectance; l) SR_B4: Band 4 surface reflectance; m) SR_B5: Band 5 surface reflectance; n) SR_B7: Band 7 surface reflectance; o) ST_B6: Band 6 surface temperature (The Landsat 8 is the 10th band); p) Elevation: Sea-level elevation.

Table A4 Classification precision of Jengish Chokusu

Year	Overall accuracy	Kappa
1990	95.7%	94.3%
1995	96.8%	95.7%
2000	97.8%	97.1%
2005	97.7%	97.0%
2010	98.1%	97.5%
2015	98.1%	97.4%
2020	96.2%	94.9%

Table A5 Classification precision of Bogeda

Year	Overall accuracy	Kappa
1990	94.4%	92.6%
1995	96.8%	95.8%
2000	98.3%	97.7%
2005	98.2%	97.6%
2010	96.7%	95.5%
2015	94.8%	92.9%
2020	95.2%	93.6%

Table A6 Classification precision of Barikun

Year	Overall accuracy	Kappa
1990	97.8%	97.0%
1995	93.5%	91.1%
2000	97.8%	97.0%
2005	98.0%	97.3%
2010	97.5%	96.6%
2015	97.5%	96.6%
2020	97.1%	96.1%